Smart Structures and Systems, Vol. 11, No. 3 (2013) 261-282
DOI: http://dx.doi.org/10.12989/sss.2013.11.3.261

A multi-radio sink node designed for wireless SHM applications

Shenfang Yuan*, Zilong Wang, Lei Qiu, Yang Wang and Menglong Liu

The State Key Lab of Mechanics and Control of Mechanical Structures,The Aeronautic Key Lab for Smart Materials and Structures, Nanjing University of Aeronautics and Astronautics, 29 Yudao Street, Nanjing 210016, People's Republic of China

(Received May 4, 2012, Revised July 25, 2012, Accepted October 3, 2012)

Abstract. Structural health monitoring (SHM) is an application area of Wireless Sensor Networks (WSNs) which usually needs high data communication rate to transfer a large amount of monitoring data. Traditional sink node can only process data from one communication channel at the same time because of the single radio chip structure. The sink node constitutes a bottleneck for constructing a high data rate SHM application giving rise to a long data transfer time. Multi-channel communication has been proved to be an efficient method to improve the data throughput by enabling parallel transmissions among different frequency channels. This paper proposes an 8-radio integrated sink node design method based on Field Programmable Gate Array (FPGA) and the time synchronization mechanism for the multi-channel network based on the proposed sink node. Three experiments have been performed to evaluate the data transfer ability of the developed multi-radio sink node and the performance of the time synchronization mechanism. A high data throughput of 1020Kbps of the developed sink node has been proved by experiments using IEEE.805.15.4.

Keywords: wireless sensor networks; structural health monitoring; sink node; multi-radio sink

1. Introduction

Structural health monitoring (SHM) is an active area of research and practice in recent years. When implementing a cable-based SHM system for large engineering structures, massive interconnections from sensors to the centralized data server require complex configurations of hardware systems which cause heavy weight of the system and the decreasing of system reliability. To solve above problems, a plenty of literatures have been published regarding applying Wireless Sensor Networks (WSNs) technology to SHM, including various nodes development, such as strain, impedance, acceleration and active monitoring nodes (Varadan *et al*. 1997, Lynch 2005, Jia *et al*. 2006, Wu and Yuan 2007, Mascarenas *et al*. 2007), energy harvesting or recharging WSN node methods (Park *et al*. 2008, Huang *et al*. 2011), evaluations of the WSN based SHM systems on bridges and aircraft structures (Lynch *et al*. 2006, Zhao *et al*. 2007, Pakzad *et al*. 2008, Wu and Yuan 2009). However, because of the limitations in terms of power, bandwidth, memory size and reliability, extensive research of WSN based SHM technology is still being conducted.

SHM is an application area of WSNs which usually needs high data communication rate to transfer a large amount of monitored data. In a typical wireless SHM application, the data

*Corresponding author, Professor, E-mail: ysf@nuaa.edu.cn

acquisitions of strain, acceleration and other parameters of the structure usually are performed at many distributed locations in real time and periodically. The fundamental frequencies of the monitored structures are around 10 Hz. However when Nyquist theorem and noise reduction algorithms are taken into account, sampling rates of several hundreds of hertz are required (Cosar *et al*. 2009). With the high sampling rate and many nodes involved, large amounts of data usually needs to be transferred to a central system to be processed. Usually, it is not possible to transmit the data immediately after sampling because of the bandwidth limitations of WSN. In SHM applications, the samples are usually stored in the memory of a sensor node and transmitted wirelessly after the sampling operation finishes. During the transmission process, these data are received by the sink node and then transmitted to a computer which has stronger processing power compared to a wireless sink node. Hence, the ability of the sink node to communicate with each cluster of sensor nodes and the attached computer plays a very important role in data collection in SHM applications. Pakzad *et al.* (2008) has reported the application of deploying a wireless sensor network consisting of 64 accelerometer sensor nodes to monitor the Golden Gate Bridge. According to their research, a complete cycle of sampling and data collection for the full network produces 20 MB of data and takes about 9 hours to transfer the data. It is the low communication ability of the sink node that constitutes a bottleneck for constructing a high data rate SHM application giving rise to such a long data transfer time. In those applications, when the monitoring has to be performed continuously, the data have to be sent to the central computer after one or several samplings to empty the memory of the sensor node. The data transfer ability of the sink node is of particular importance. An example of this application scenario is the structure strain monitoring requested in the F35 Prognosis and Health Management (PHM) project. The sampling rate needed is 320Hz and the data is required to be recorded continuously (Timothy *et al*. 2009).

A lot of researches have been performed to improve the data transfer ability of the sink node. Cosar *et al*. (2009) proposed a new wireless sink node to convert the data received from the network into analog signal levels, which are sampled through the data acquisition board connected to a PC and the original data is reconstructed offline later. This method can improve the speed to transfer data from the sink node to the computer, but can not improve the data throughput from the sensor nodes to the sink node. Multi-channel communication has been proved to be an efficient method to improve high data throughput problem by enabling parallel transmissions over different frequency channels (So and Vaidya 2004, Bahl *et al*. 2004, Marina *et al*. 2005, 2010, Raman *et al*. 2007, Avallone *et al*. 2009, Campbell *et al*. 2010, 2011, 2011, Kuo and Fitch 2011). Methods to realize the multi-channel communication can be divided into two kinds. The first one is the single radio solution (So and Vaidya 2004, Campbell *et al*. 2010, 2011). Campbell *et al*. (2010, 2011) studied the multi-channel communication method based on the 802.11 DCF over a single radio in order to improve its communication performance on throughput, end-to-end delay. They proposed an algorithm to allow a node access to multiple non-overlapping channels dynamically through channel switching. But they observed that the presented algorithm performed poorly when receiving data at the sink node because the single radio had to be constantly switched to different channels. Marina *et al*. (2010) also mentioned that because the fast channel switching capability was not yet available with commodity hardware and the tight time synchronization was requested among nodes, the single radio solution was not practical under many application scenarios. The other kind of methods is multi-radio solution (Bahl *et al*. 2004, Marina *et al*. 2005, 2010, Raman *et al*. 2007, Avallone *et al*. 2009, Campbell *et al*. 2011, Kuo and Fitch 2011). Bahl *et al*. (2004) discussed the significant benefits of capacity enhancement in wireless systems offered by using multi-radio platforms. Campbell *et al*. (2011) discussed several methods to realize the

multi-channel multi-radio data transfer method including multiple sinks with single radio, single sink with multiple radios, single sink with multi-radios and multiple sink with multi-radios. They were demonstrated through simulations that if the radio switching between channels was eliminated and data flowing could be received constantly from senders to the receiving radio interfaces, the performance at sink node could be greatly improved. Kuo and Fitch (2011) reported a modular robot equipped with multiple sinks with single radio. They presented a hardware implementation to connect six Microchip 2.4 GHz IEEE 802.15.4 modules to a custom STM32F microprocessor board. The multi-radio solutions have been proved to be effective to solve the problems of sensor networks encountered when high data throughput is needed.

To realize the multi-radio solution, some approaches to develop the single node with multi-radio ability have been reported recently (Kohvakka *et al*. 2006, Zurich 2007, Lymberopoulos *et al*. 2008, Gummeson *et al*. 2010, Popovici *et al*. 2011, SHIMMER Research 2011, Jurdak *et al*. 2011). However, most of the node implemented only with 2 radios. Kohvakka *et al*. (2006) reported the approach of 4 radio implementation based on the IEEE 802.11. Though the 802.11 based radios provide higher data rates, they come with higher power consumption as well. In the application area of SHM, considering of the low energy consuming request, a large percentage of wireless sensor nodes now applied use a radio which conforms to the IEEE 802.15.4. Considering this, this paper proposes a multi-radio integrated sink node design method based on the Field Programmable Gate Array (FPGA) and IEEE 802.15.4 for parallel communication in wireless structural health monitoring system. Using the presented method, an integrated sink node with 8 radios working parallel is developed. It provides a large network throughput at the sink node compared to ordinary IEEE 802.15.4 radio based WSN nodes. When more RF radios are adopted in the sink node, the process of encoding, decoding and error detection/correction in the FPGA will be more complicated. Special software caching mechanism and high-speed data transfer mechanism have to be designed.

The structure of this paper is as follows: Section 1 gives the brief introduction of the research presented. Section 2 proposes the design method of the multi-radio sink node. FPGA is applied as the Micro Control Unit (MCU) which controls several RF modules. The FPGA module also realizes caching mechanism to standardize data encapsulation to gather data from multiple channels, and controls Universal Serial Bus (USB) 2.0 bus to transmit data with high-speed and in real-time from the sink node to the monitoring center. Section 3 presents the hardware and software development of the 8-channel multi-radio sink node. It can receive data from 8 channels provided by IEEE802.15.4 protocol simultaneously. A double-layer parallel-to-serial data caching mechanism is designed. To reduce the time spent on data processing and transmission, a high-speed data transfer mechanism is presented by building parallel private processing units. Section 4 presents the time synchronization mechanism for the multi-radio sink node based WSN. Section 5 establishes three experiments to evaluate the data transfer ability of the developed multi-radio sink node and the performance of the time synchronization mechanism.

2. Design method of the multi-radio sink node

The hardware structure of the proposed parallel communication sink node is shown in Fig. 1. Different from ordinary sink node, this node consists of multiple independent RF radios, the FPGA, the USB chip, the Electrically Erasable Programmable Read-Only Memory (E2PROM), the power management module and the clock module. It is the high-speed parallel working ability of FPGA

chip that is adopted to control several RF modules to receive data packets from different channels simultaneously. It also processes received packets by operating mechanisms such as High Level Data Link Control (HDLC) and Cyclic Redundancy Check (CRC), and then transmits data streams to monitoring center through USB2.0 port in real time. HDLC and CRC are two mechanisms usually adopted during communication between two nodes to ensure a correct data transfer (IEEE Std 802.15 2003).

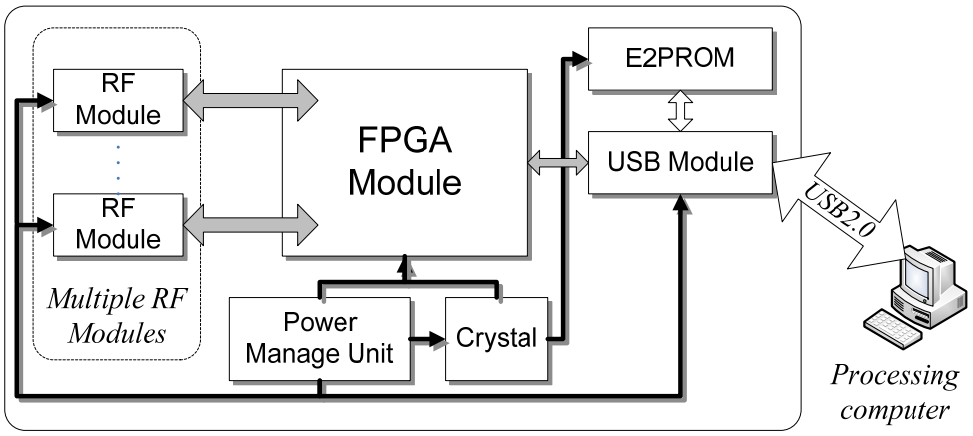

Fig. 1 Hardware structure of the proposed sink node

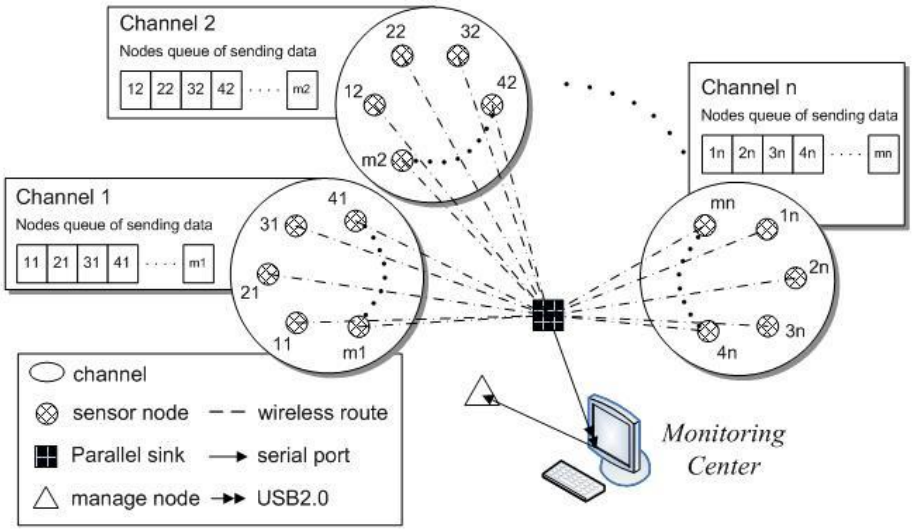

Fig. 2 Topology of the multi-radio sink node based WSN system

Fig. 2 shows the topology to construct a wireless SHM system based on the presented multi-radio sink node. In the network, the wireless SHM nodes are arranged into several clusters in different structure locations. To avoid conflictions, each node cluster works in a channel which is provided by IEEE802.15.4 protocol, labeled as Channel *n* in Fig. 2. There are totally 16 different available channels. A management node in the network is designed to start, suspend and stop the operation of sensor nodes and also keep the time synchronization for the whole network. During the working state, the proposed multi-radio single sink node receives data packets from multiple clusters which work in multiple communication channels simultaneously.

Although the sink node includes multiple channels, these channels transfer data packets independently. Since each cluster works in different channel, the data collision from different clusters can be avoided.

According to IEEE 802.15.4, the largest data transmit rate of the radio hardware is 250Kbps. Because there are multiple channels in the network, the instantaneous data transmit rate of the whole network can be multiple times of the rate that can be provided by the network based on the single radio sink. When the network uses 16 channels, the fastest possible network instantaneous data transmit rate is 4Mbps. Since the USB2.0 mechanism can support 12Mbps data throughput which is more than 4Mbps, the extreme network instant data transmit rate, the multi-radio sink node is completely able to upload data to central computer system in real-time.

3. The sink node development

In this paper, a multi-radio sink node with 8 RF modules is developed as the illustration of the presented sink node design method. The development includes hardware and software.

3.1 Hardware design of the proposed sink node

The FPGA adopted should be chosen according to following aspects: (1) It should have a sufficient number of available I/O pins; (2) It should support high enough crystal frequency for working; (3) The size of the FPGA chip should be small; (4) The resource of the FPGA chip should be enough. In this design, the FPGA chip EP3C16Q240C8N from ALTERA Company is chosen. This chip contains 240 pins which are enough to connect 8 RF modules. It operates at 50MHz with 64KB Random Access Memory (RAM) which is suitable to program the software of the developed sink node.

CC2420 RF module from Texas Instruments (TI) is chosen as the radio module in the design. To control one CC2420 RF module, FPGA configures four available Input/Output (I/O) pins to receive working condition of CC2420 RF module and another four available I/O pins as analog Serial Peripheral Interface (SPI) to exchange data with CC2420, send commands to CC2420 and access internal registers and storage of CC2420.

The FX2 CY7C68013 from CYPRESS is chosen as the USB2.0 chip. CY7C68013 chip has two interface modes: (1) Slave First-In-Firs-Out (FIFO) mode; (2) General Programmable Interface (GPIF) mode. In this paper, it works in the Slave FIFO mode. In this mode, FPGA can read and write the FIFO buffer in CY7C68013 chip in the same way as operating an ordinary FIFO.

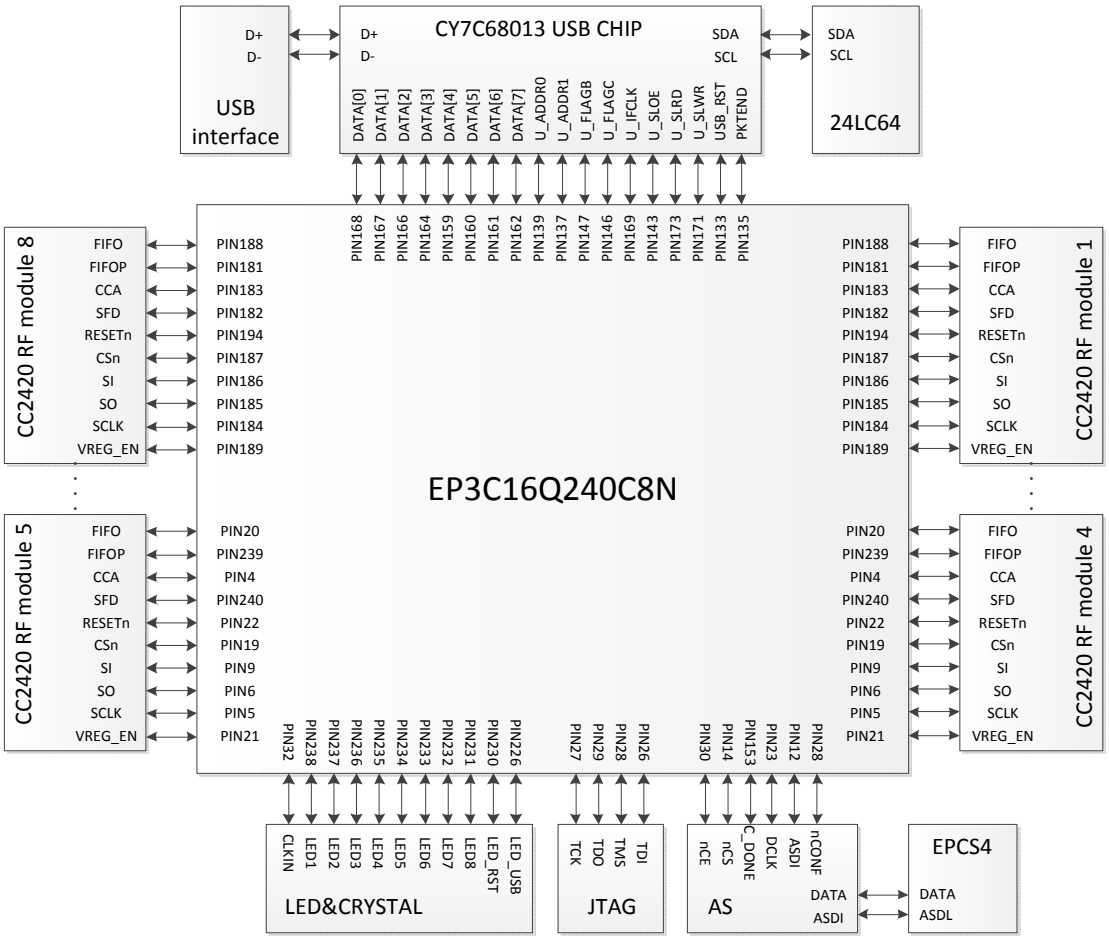

Fig. 3 Schematic design of the 8-radio sink node

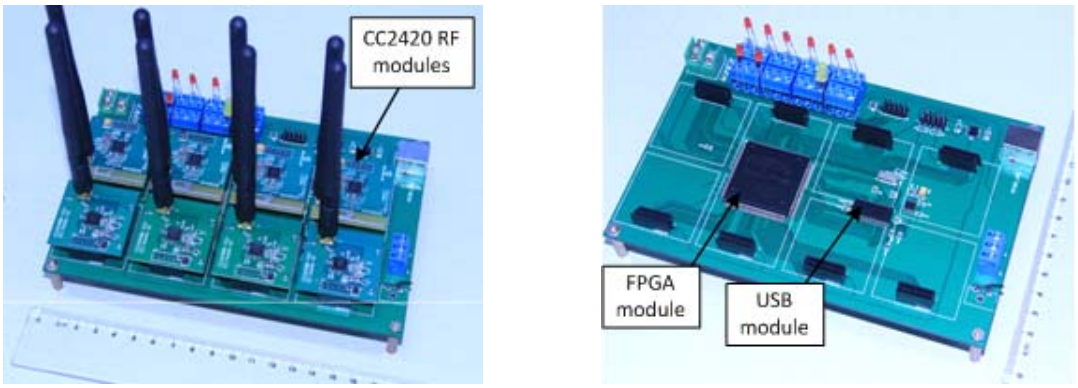

(a) sink node with 8 RF modules (b) sink node without RF module

Fig. 4 The developed 8-radio sink node

Fig. 3 is the schematic design of the 8-radio single sink node. Fig. 4 is the developed 8-radio sink node with size of 18 cm×11.5 cm. Because the sink node is used near the central computer system in the WSN application, no strict weight and energy consumption limitation exists for the service of this kind of node. The size of the developed node is reasonable.

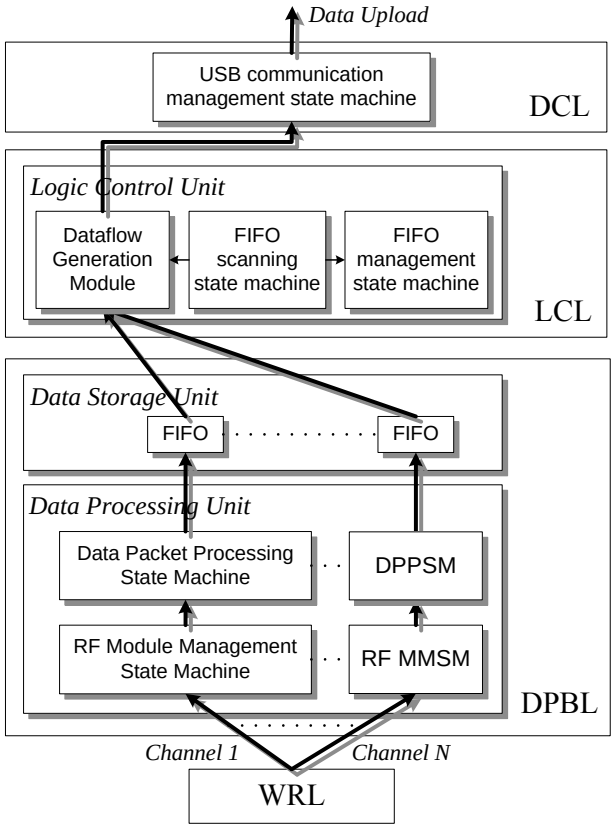

Fig.5 Software structure of the developed sink node

3.2 Software design of the sink node

Fig. 5 shows the software structure of the developed sink node. To manage the encoding, decoding and error detection/correction when data are received from multiple RF radios, a double-layer parallel-to-serial data caching mechanism and a parallel private processing units based high-speed data transfer mechanism are designed. The software structure is built with wireless receiving layer (WRL), data processing buffer layer (DPBL), logic control layer (LCL) and data communication layer (DCL) from the bottom to the top layer.

The double-layer parallel-to-serial data caching mechanism first builds multiple special sub-FIFOs as data caching units in DPBL in the parallel caching layer. Then, in the serial caching layer, a main FIFO unit is built in DCL to gather the data in sub-FIFOs for uploading.

The high-speed data transfer mechanism is designed by building two kinds of private processing units, named as RF module management state machine and data packet processing state machine in DPBL for each communication channels. When the sink receives data from different radios, the software distributes the data to their corresponding private processing units. These processing units work parallel to process the data. Using this mechanism, less time is consumed comparing to ordinary queue processing mechanism. The data processing speed can be improved greatly.

DPBL contains data processing unit and data storage unit. Data processing unit includes RF module management state machine and data packet processing state machine. RF module management state machine is used to control the single connected RF module. The main functions include: (1) initializing the RF module when power is on; (2) responding to the interrupt signal from the RF module when it receives a data packet and driving the state machine to read the received data packet from RXFIFO; (3) resetting RF module when an error happens. Because multiple units are designed to every RF module separately, the sink node can control these RF modules parallel and handle every data packet receiving interrupts fast at the same time. The main functions of packet processing state machine include: (1) processing the data packet according to the HDLC protocol; (2) adding CRC code at the tail of the packet for the monitoring center to check the incorrect data transmission; (3) storing the processed data packets into the corresponding FIFO of data storage unit. The data upload process of the developed sink node is different from traditional ones. At first, data is formed into a stream and then the data stream is uploaded on the monitoring center. The monitoring center cut the data stream to data packets by separating packets with 0x7E according to the HDLC protocol, parsing data packets and obtaining the information.

Many FIFO internals are built in the FPGA to constitute the data storage units. Each data channel contains a FIFO which is used to receive and cache the processed data packets. The read-enable of a FIFO is controlled by the logic control unit, while the write-enable is controlled by both the data processing unit and the logic control unit. When the logic control unit reads data from one FIFO, write-enable is turned off until this FIFO is completely empty. In this process, if the CC2420 RF module receives a data packet, this packet is temporarily stored in the Receive FIFO (RXFIFO) of CC2420 RF module to avoid the conflictions and errors which are caused by reading and writing FIFO at the same time.

LCL includes FIFO scanning state machine, FIFO management state machine and dataflow generation module. The FIFO scanning state machine constantly scans every RF module and connects the FIFOs one by one. Meanwhile the FIFO management state machine controls these FIFOs according to the scanning result. By merging and reducing the time which is spent on reading data packets in different RF modules and processing the data flow, the design of multiple FIFO internals and LCL resolves the contradiction between low RF modules working efficiency with the intention of improve network throughput.

DCL contains the USB communication management state machine which connects the USB chip with FPGA and provides data transmission channels and manages the software interface of USB. This state machine controls the dataflow generation module, sends data to the cache FIFO in the USB chip with a high-speed and waits for a bulk upload to the monitoring center when data are read out from the data storage unit.

The workflow of sink node is shown in Fig.6. Fig. 6 (a) shows the data reception and storage process of every channel. It shows the workflow in DPBL in Fig. 5. Fig. 6 (b) contains two closed cycles. The left one presents the cooperation of many channels in DPBL. The right one shows the workflow of LCL. It presents the data upload workflow chart of the 8-radio sink node by

combining both figures. When the sink node begins to work, the multiple RF modules parallel receive wireless data packets from their own channels respectively. When one of the RF modules receives a packet, the data processing unit reads it from the RXFIFO in DPBL connecting to this module. The packet is stored in the FIFO of data storage unit after it is processed by the HDLC protocol and added the CRC check code. Meanwhile, the other RF modules work independently. Logic control unit in LCL checks each FIFO of data storage unit circularly. When data storage is found in a FIFO, the action of data processing unit connected with this FIFO is suspended, and the stored data are read out immediately. USB communication management state machine in DCL controls USB data bus to store the data in the cache FIFO on USB chip. At last, the USB chip uses bulk transfer mode to upload data to the monitoring center.

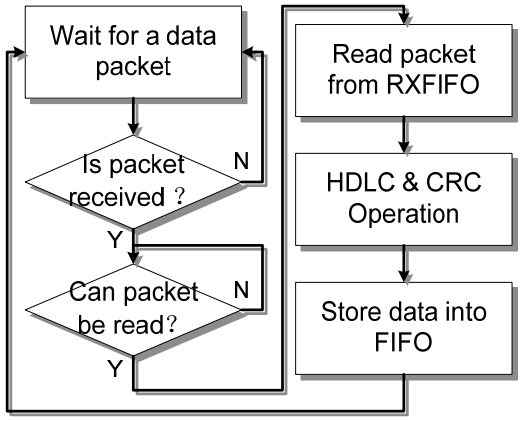

(a) Reception and storage of each channel data in DPBL

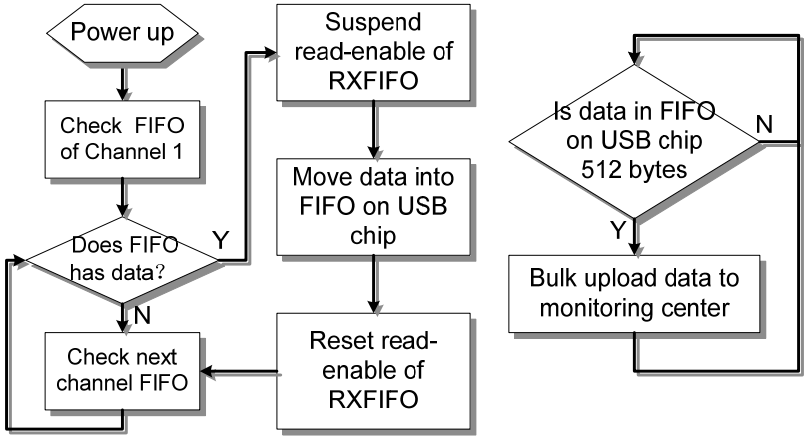

(b) Data upload workflow chart in DPBL and LCL

Fig. 6 Workflow paths of the 8-radio sink node

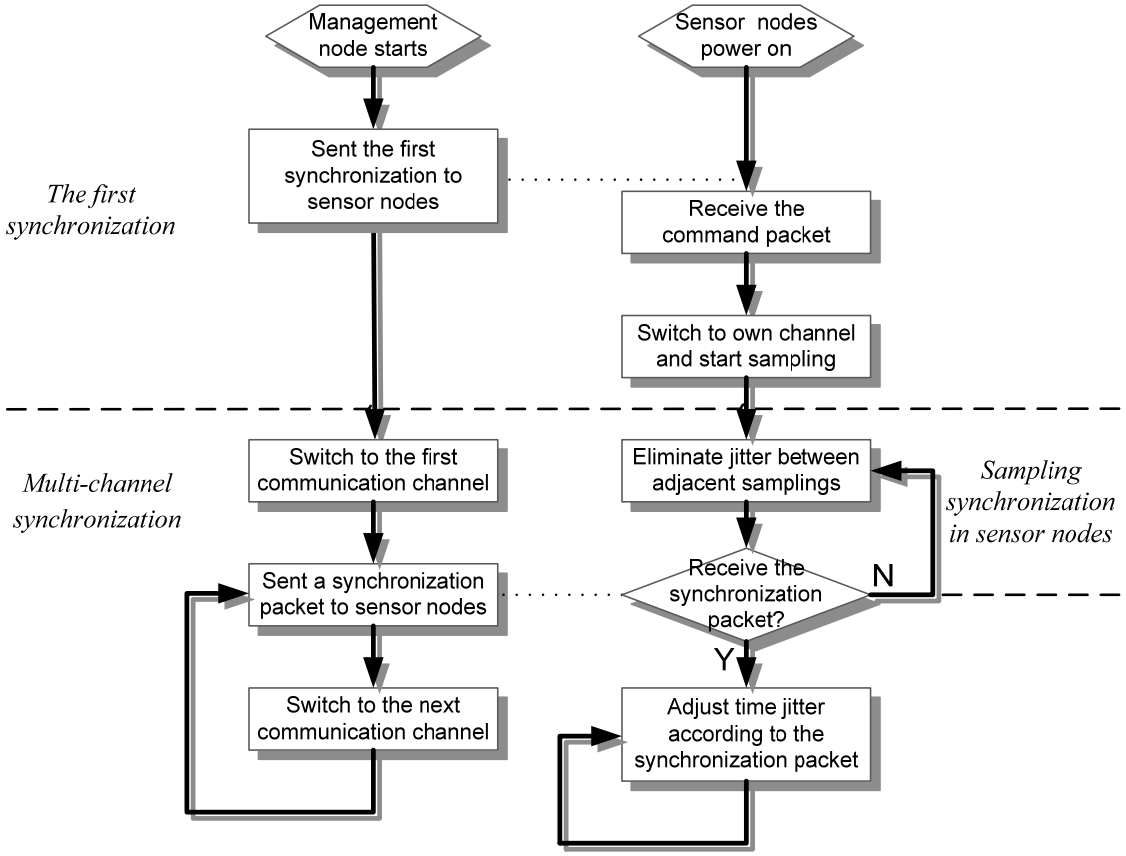

Fig. 7 The designed multi-channel synchronization mechanism

4 Time synchronization implementation for multi-radio sink based WSN

Fig. 2 shows the topology of the proposed multi-radio sink node based WSN system. When the network is organized, besides the sink node and sensor nodes, another ordinary WSN node is adopted to be the management node. This node is adopted to coordinate the activities of the network and also perform the network synchronization.

The synchronization mechanism design is shown in Fig. 7. Before the whole network begins to work, every node is switched to work in the same communication channel. The management node performs a first synchronization of the whole network. After this process, each sensor node switches to its own working channel and begins the sampling process. During the working process, the management node switches to each channel in sequence and perform the synchronization of the nodes working in this channel. The job is designed to de done in a fixed interval which is decided by the synchronization request. Besides this multi-channel synchronization mechanism, another mechanism is also designed for each node to compensate the sampling trigger difference at each data sampling process to ensure the sampling synchronization. The detail design of the synchronization mechanism is presented in this section.

4.1 Multi-channel synchronization mechanism

When the management node switches to one channel, it performs the synchronization using a process shown in Fig. 8. The management node sends out a synchronization packet with its own clock time stamp T_{01}. Each sensor node works in this communication channel receives this packet, and records its own clock time stamp T_{11}. When next synchronization action is performed, similarly, the time stamp of the management node T_{02} and the corresponding time stamp of the sensor node T_{12} are recorded. The clock time difference between the management node and the sensor node then can be calculated by Eq.(1)

$$\mathrm{T_{MN}} - \mathrm{T_{SN}} = (T_{02} - T_{01}) - (T_{12} - T_{11}) \tag{1}$$

The sensor node corrects its clock time for next sampling according to Eq. (1). After sending the synchronization packet in this channel, the management node switches to another channel and performs the same process. After all channels are switched, one round of multi-channel synchronization is finished. The management node performs this synchronization at a fixed interval continuously.

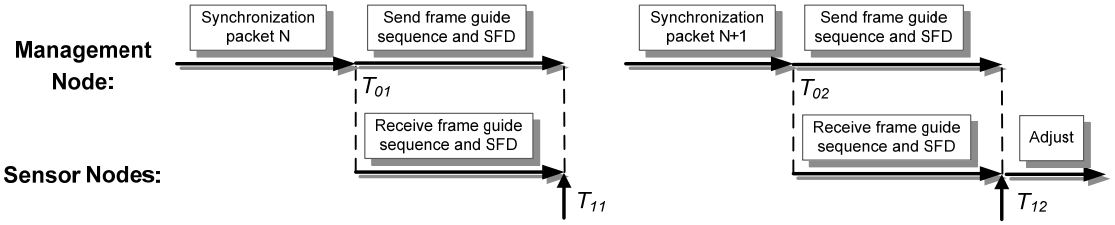

Fig. 8 Time synchronization process between the management node and sensor node

4.2 Sampling synchronization mechanism in the sensor node

The data sampling at each node is triggered by a timer on the node. According to the data sampling frequency requested, a count value is usually calculated for the timer to trigger the sampling task. Let N_S represent this count value. After N_S count, the timer is supposed to trigger the sampling task. However, since the sampling task of the node has some random influence by other running tasks which occupy the control of the processor, the sampling trigger can not be ensured to be performed at exactly N_S count. This error can continuously accumulate to an extent to influence, the synchronization of the whole network. A sampling synchronization mechanism is put forward to reduce this error of sampling trigger.

This sampling synchronization mechanism can be described as following: (a). If last count in the timer to trigger the sampling in the sensor node is $N_{S,}$ the trigger counter is still set to be N_S at this sampling. (b). If last count is $N_s + x$, the trigger counter is set to be $N_s - x$ this time. (c). If last count is $N_s - x$, the trigger counter is set to be $N_s + x$ this time. This compensation

mechanism can ensure the sampling trigger time does not have a big difference giving rise to a small synchronization error.

5. Evaluation experiments

Three experiments are performed to evaluate the performance of the developed multi-radio sink node and the performance of the time synchronization mechanism.

5.1 Data throughput evaluation experiment

In this section, an evaluation experiment is performed to test the data throughput supported by the multi-radio sink node. In order to compare with ordinary IEEE802.15.4 node's ability, the baseline data throughput between two single-radios is discussed first. A number of researches and experiments have been performed to evaluate the base line maximum data throughput between two IEEE802.15.4 single-radio nodes (Osterlind and Adam 2008, Jurdak *et al*. 2011). Though the transmit rate of the radio of IEEE 802.15.4 is 250Kbps, Osterlind and Adam (2008) prove that the maximum throughput of the radio is 225Kps because of the difference accounted for the interframe spacing and preamble bits required by hardware. And if the packet copying is performed between the radio receiver and the microcontroller which is usually necessary during real data sampling and sending procedure, the maximum data throughput can be reached is only around 140Kbps. Jurdak *et al*. (2011) reported the maximum data throughputs of radios on different wireless platform, including 51.2Kbps of TelosB and 114.2Kbps of Iris.

In the experiment performed in this paper, besides the developed multi-radio node, 8 TelosB nodes with MSP430 microcontroller and CC2420 radio chip on are adopted to send data to the multi-radio node, which is similar in Osterlind and Adam (2008) and Jurdak *et al*. (2011). The software in the central computer is designed based on Labview. Its function includes receiving data which is uploaded by the multi-radio sink node and calculating the number of the received data bytes. In order to evaluate the maximum throughput, these data received are not stored in the computer. Fig. 9 shows the throughput evaluation experiment system.

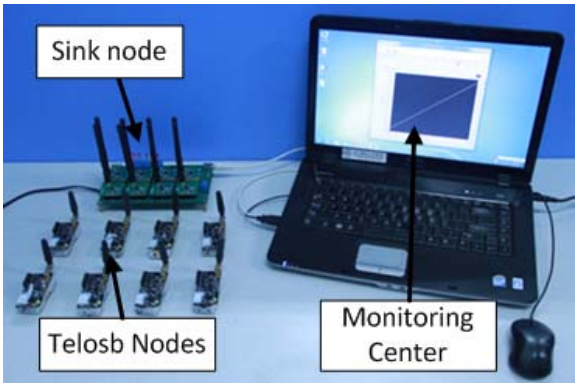

Fig. 9 Data throughput experiment setup

Because there are 16 communication channels provided by IEEE 802.15.4 protocol, in order to reduce the mutual interference among different channels, in the experiment, only odd numbered channels are adopted, namely Channel 11, 13, 15, 17, 19, 21, 23 and 25. Under this situation, every adopted channel can keep at least one channel interval with other used channels. To distinguish data packet sources clearly, these channels are relabeled as Channel 1 to 8 respectively corresponding to RF module 1 to RF modules 8 of multi-radio sink node. The TelosB nodes are programmed to send data packets to the multi-radio sink node at the same setup as reported in Osterlind and Adam (2008). The Clear Channel Assessment Mechanism (CCA) is adopted. Its threshold value is set to the typical value of -77 dBm. Fig. 10 (a) shows the software initialization process of the TelosB node. When its CC2420 registers are configured, the mechanisms which may influence the largest network data throughput realization, such as the address recognition function and in-line security operations are disabled.

After initialization of the TelosB node, a fixed packet is written directly into the transmit FIFO (TXFIFO) of the CC2420 chip on the TelosB node. The size of the fixed packet is 126 bytes, consisting of 1-byte of frame length, 2-byte of frame control field (FCF), 1-byte of data sequence number, 6-byte of address information and 116-byte of 0x00 bytes. Another 2-byte frame check sequence (FCS) is achieved by CC2420 hardware which is put at the end of the whole packet. Therefore, the data packet is 128-byte. The data packet transmitting process is shown in Fig. 10 (b).

In order to test the maximum data throughput of the multi-radio sink node, the program of the multi-radio sink node is a little different from what is introduced in the section 4. HDLC and CRC mechanisms used for checking USB communication are disabled.

During the experiment, data throughputs when different numbers of TelosB nodes are activated to send data respectively from 1 to 8 are tested. The experimental network throughputs obtained are shown in Table 1. Fig. 11 shows the relationship between the throughputs reached with the number of radios adopted. The maximum throughput when only one channel is used is 135Kbps which is similar to the maximum throughput of 140Kbps reported in Osterlind and Adam (2008). When all the 8 radios are used together, the maximum throughput can reach 1020Kbps which is significantly improved compared to the maximum data throughput of ordinary IEEE 802.15.4 radio sink node.

Though from the theory analysis, the multiple channel method based on multiple sinks with single radio can have similar data throughput as the developed multi-radio sink node, multiple sinks have to occupy multiple USB ports of the central computer and the system is not compact.

5.2 Strain monitoring experiment setup

In order to further prove the parallel working ability of the developed sink node, a WSN monitoring system with 50 leaf nodes is constructed. As shown in Fig. 12, the experimental wireless sensor network is built by two parts. The first part is a strain monitoring system which is used to monitor the strain distribution on an epoxy-glass composite plate whose size is 70 cm×70 cm. 25 foil gauges are attached on it and connected to 25 sensor nodes. Fig. 13 shows the strain wireless sensor node adopted which are developed by the authors' group (Wu and Yuan 2007). Each node contains four sampling channels with 10-bit sampling resolution. In the experiment, although only one sampling channel is connected with the strain gauge, the data packet includes all data from the four sampling channels which are provided by the sensor node. The data of the other three sampling channels are set to zero. In order to evaluate the ability of the developed sink node

in a large scale, another 25 nodes are also adopted in the experiment without strain sensor platform patched. In the experiment, they just send fix data packets to the sink node. In addition, as shown in Fig. 12, a two channel DPM-912A strain indicator from KYOWA Company is adopted to verify the function of the strain monitoring system.

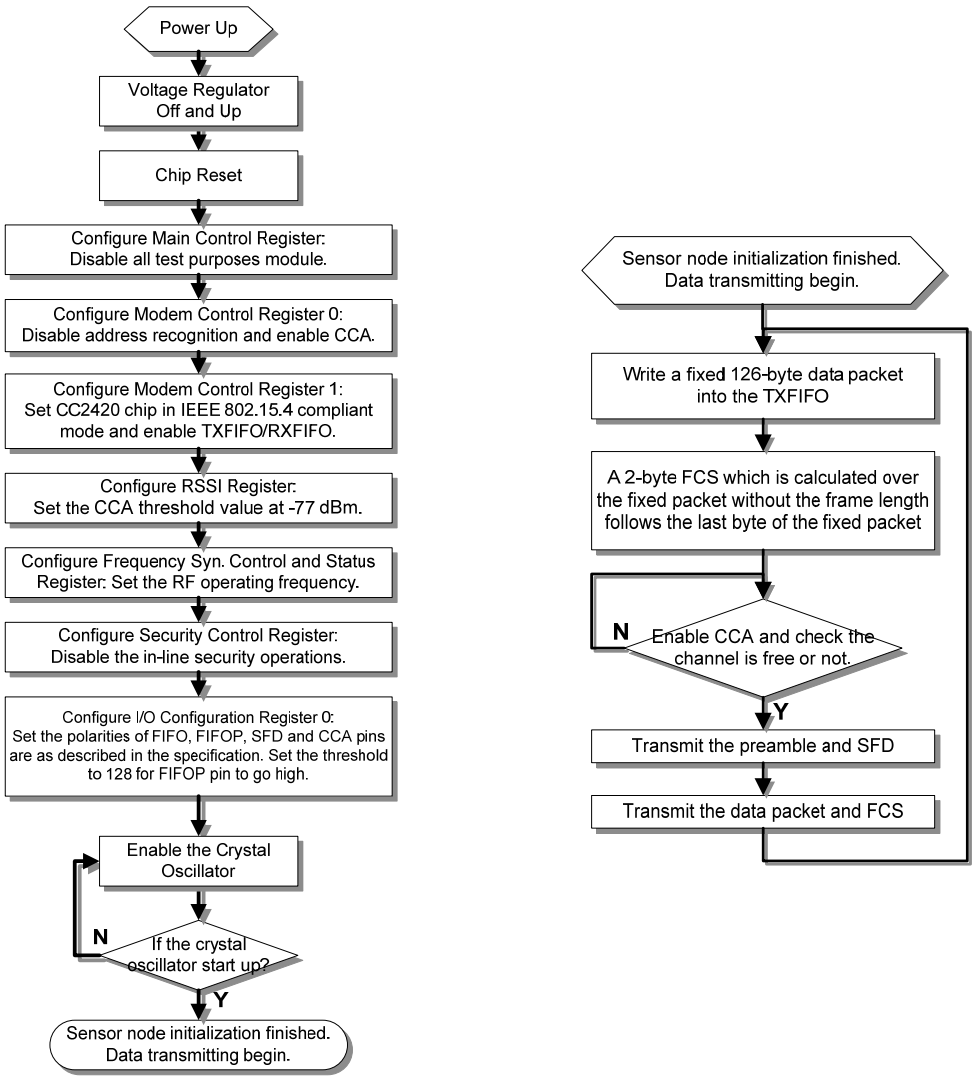

(a) Initialization process of the TelosB node (b) The data packet transmitting process

Fig.10 Data transmitting software in TelosB node

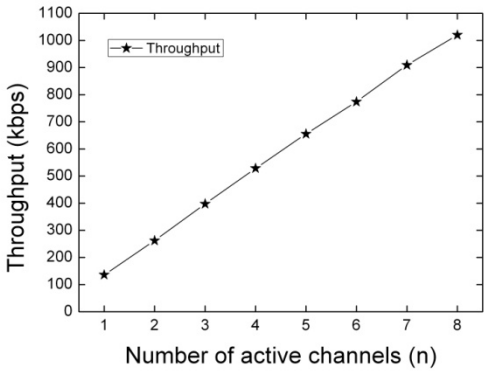

Fig.11 Experiment results of the sink node throughput evaluation experiment

Table 1 Data throughput evaluation results of the multi-radio node

Number of Channels	Throughput (Kbps)
1	135.7
2	262.2
3	397.3
4	528.4
5	655.4
6	774.1
7	909.3
8	1020.0

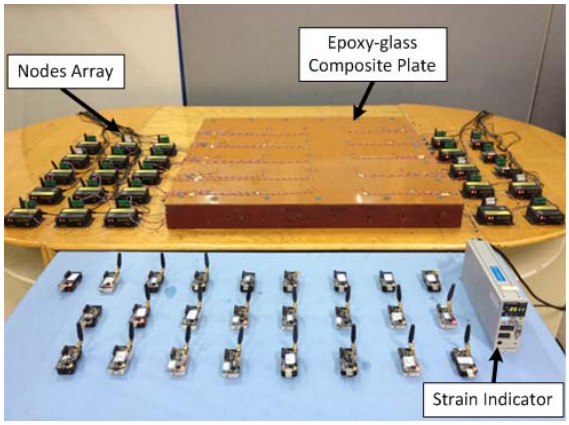

Fig. 12 Strain monitoring wireless network in the experiment

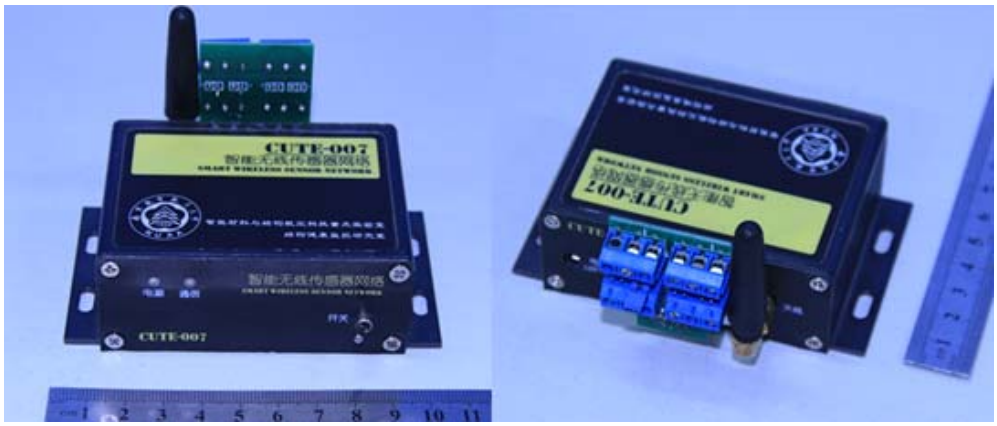

Fig. 13 Strain wireless sensor node adopted

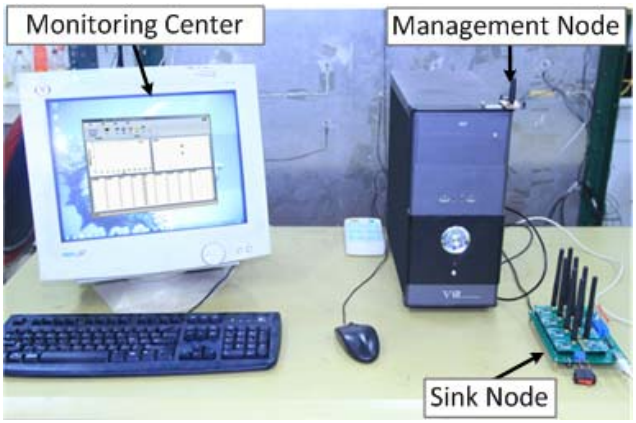

Fig. 14 Monitoring center setup of the experiment

These 50 nodes are arranged into 8 clusters which work in individual communication channels. 7 nodes are grouped as a cluster to work in Channel 1 and Channel 2 respectively. In every other channel, 6 nodes are grouped as a cluster. To distinguish these nodes, an identify (ID) number is given to each node according to its index in the cluster and communication channel used. For example, No.21 node means the second node in the cluster working in Channel 1. Fig. 14 shows the monitoring center which is attached with the multi-radio sink node. Through a software interface developed for this experiment, the behavior of each sensor node and the monitoring data of each strain gauge can be shown in real time. Fig. 15 shows the arrangement of the strain gauges on the composite plate. When a load is applied on a certain area on the plate, the strain distribution of the whole plate are changed and can be monitored by the WSN nodes. If the communications in different channels are performed successfully, the strain monitoring results can be shown simultaneously on the software interface. In the experiment, the strain monitoring is designed to be a continuous one which is requested in many SHM application scenarios. The sampling rate of

each node in this experiment is set to 32 Hz. After 8 sampling periods, the data is packed and sent to the sink node by each sensor node. The data packet is 82-byte long including the data defined by IEEE 802.15.4 and MAC Protocol Data Unit (MPDU). The MPDU contains the information of previous access network identifier (PANID, 4-byte), channel number (2-byte), node number(2-byte), sampling data (64-byte), reserve bytes (2-byte), sequence number (3-byte) and frame checkout sequence (FCS, 2-byte).

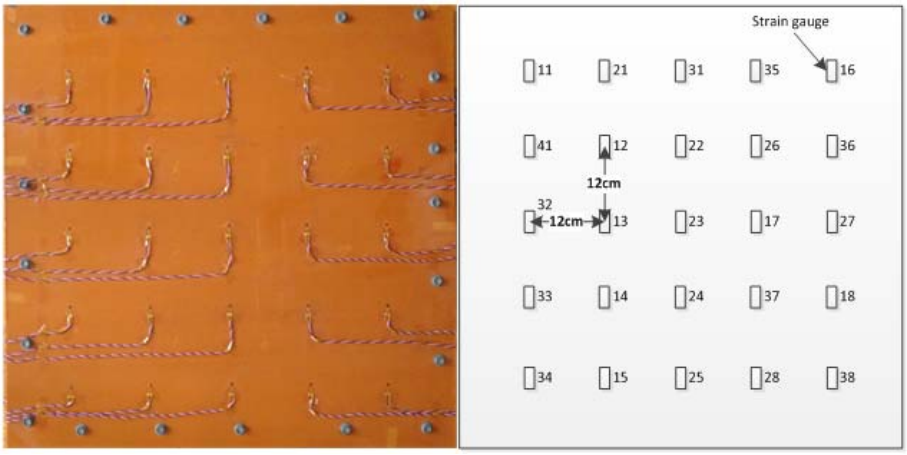

Fig. 15 Arrangement of the strain gauges

Fig. 16 shows a typical test result. 25 curves from 25 strain nodes are obtained successfully. Every curve presents a strain value from one strain gauge attached on the structure. Each plot value is an average of 20 sampling data. At the beginning of the experiment, since no load is applied, the strain values are zero. At time 65s, a load is applied on the structure. All the 25 strain nodes have simultaneous outputs. Since at different positions on the structure, different strains are caused, the output of each WSN node is different from each other. At time 88s, the load is removed, the network monitors the change and each node again presents this change at the same time. Besides the WSN strain nodes, data from the other WSN nodes which are fixed data are also received successfully by the central computer system through the developed sink node. The monitoring experiment is continually performed for 3 hours without failure. After the strain monitoring experiment, No.17 and 23 strain gauges are connected to the DPM-912A strain indicator. The loading process is repeated. The testing results are compared to the results obtained by WSN nodes, shown in Fig. 17. The strain data obtained are almost the same.

These results further prove the multi-channel simultaneous communication ability of the developed multi-radio sink node.

5.3 Time synchronization evaluation experiment

In this section, an evaluation experiment is performed to test the performance of the proposed time synchronization mechanism. To accurately measure the sampling time difference among sensor nodes, an arbitrary waveform generator (AWG) is adopted to generate a fixed waveform for

the sensor nodes to sample synchronously. The synchronization error among these nodes can be analyzed according to the relationship between the voltage and the time of the signal fed to the nodes.

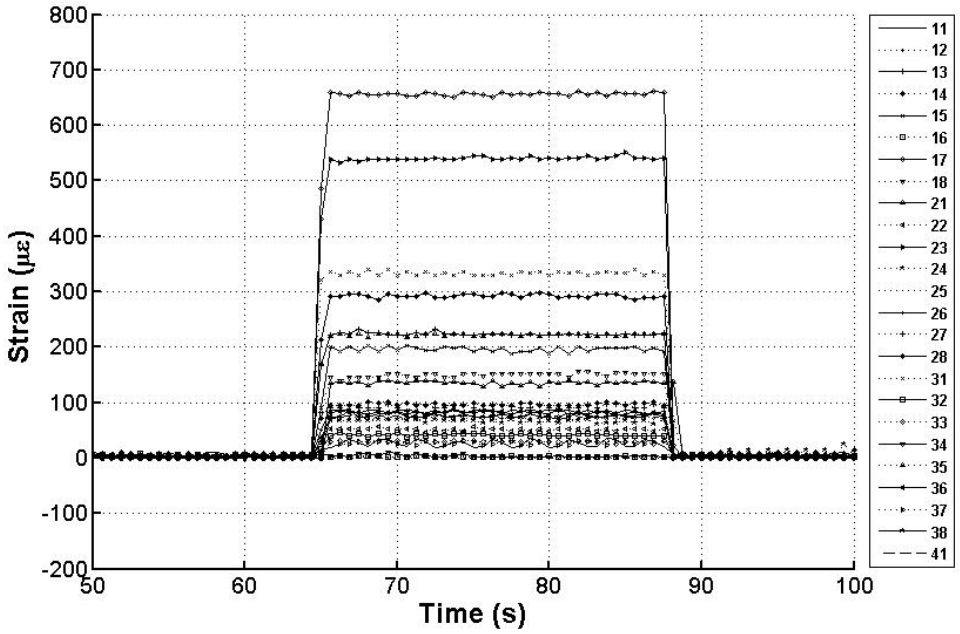

Fig. 16 Strain monitoring results from 25 nodes in 8 channels

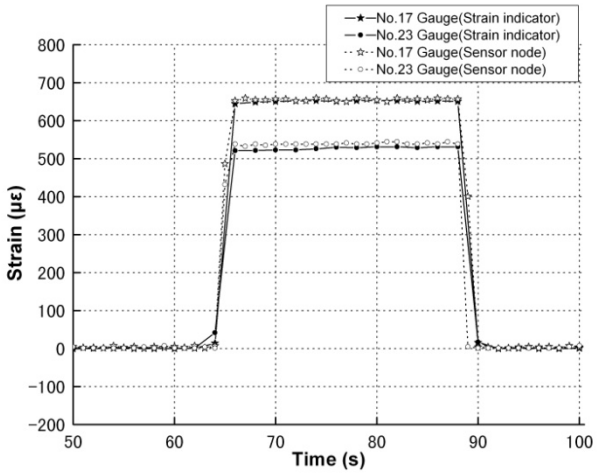

Fig. 17 Strain monitoring results by No.17 and 23 strain gauges

The experiment system includes the multi-radio sink node, 16 TelosB nodes used as sensor nodes, 1 TelosB used as the management node, a laptop and an AFG3021 AWG. The output precision of the adopted AWG is 14-bit. The experiment system is shown in Fig. 18. These 16 nodes are averagely arranged into Channel 1 to 8. The output of the AWG is connected with the ADC0 and GND pins of all the 16 nodes. A triangular wave is adopted as the input signal. The voltage range is set to 0-2.5Vand the slope of the rising side is set to 300V/s. Because the range of ADC0 is set to 0-2.5V and it is a 12-bit A/D converter, a unit of sampling data value equals to 0.61mV and corresponding to 2μs in the rising side of the input signal. Therefore, by observing the sampling data from all sensor nodes at the same sampling time point during the rising period of signal, the difference of time synchronization can be calculated.

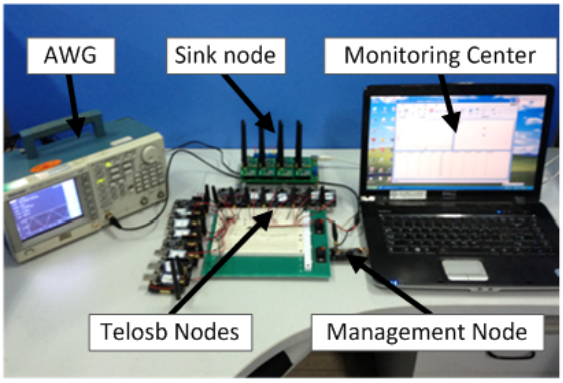

Fig. 18 Time synchronization experiment setup

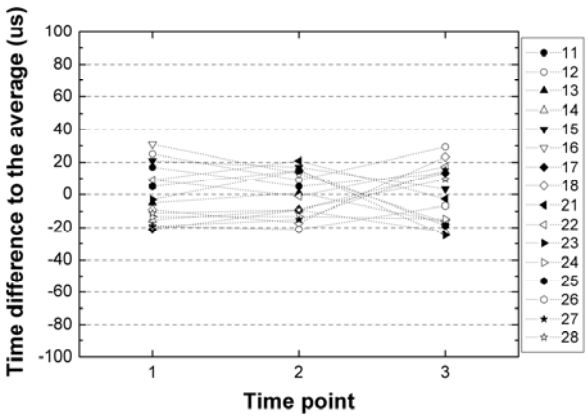

Fig. 19 Synchronization experiment results

Table 2 Sampling voltage difference and the corresponding time difference

Node Number	Voltage (V)		
	1	2	3
11	0.8734	0.9283	0.9979
12	0.8759	0.9296	1.0028
13	0.8667	0.9271	0.9888
14	0.8636	0.9241	0.9869
15	0.8746	0.9320	0.9949
16	0.8777	0.9308	0.9888
17	0.8618	0.9241	0.9979
18	0.8655	0.9216	1.0010
21	0.8710	0.9332	0.9930
22	0.8710	0.9265	0.9991
23	0.8673	0.9314	0.9863
24	0.8643	0.9229	0.9894
25	0.8698	0.9314	0.9882
26	0.8624	0.9204	0.9918
27	0.8624	0.9222	0.9985
28	0.8649	0.9241	0.9967
Average	0.8683	0.9269	0.9939
Max	0.8777	0.9332	1.0028
Min	0.8618	0.9204	0.9863
Δ (Max-Min)	0.0159	0.0128	0.0165
Time difference (us)	52	42	54

In the experiment, the time synchronization interval is chosen to be 10s to target a synchronization precision around 50μs. 10s is decided by estimating the node's crystal drift. All the nodes adopted using a DT-26 32.768KHz external crystal from DASHINKU Corp (KDS) with a frequency stability of 5ppm at room temperature. The possible crystal drift is around 50μs after 10s. Hence 10s is chosen to be the synchronization interval. The sampling results for 16 nodes at three time points are shown in Table 2. The time synchronization differences are shown in Fig. 19. According to the experiment result, the sampling synchronization error using the presented synchronization mechanism is around 50 μs which is reasonable for SHM applications. (Kim *et al*. 2007).

6. Conclusions

To solve the bottleneck problem of the sink node for constructing high data rate SHM applications, this paper proposes a design method of multi-radio integrated sink node based on IEEE.805.15.4. A high data throughput of 1020Kbps of the developed 8 radio sink node has been proved by experiments. A synchronization mechanism is also presented to synchronize the multi-radio sink node based WSN. This kind of sink node shows its important potential in constructing high performance WSN based SHM applications.

Acknowledgements

This work is supported by the Natural Science Foundation of China (Grant No. 51225502, 50830201), Seventh Framework Program (Grant No. FP7-PEOPLE-2010-IRSES-269202) and the Priority Academic Program Development of Jiangsu Higher Education Institutions.

References

Avallone, S., Akyildiz, I.F. and Ventre, G. (2009), "A channel and rate assignment algorithm and a Layer-2.5 forwarding paradigm for multi-radio wireless mesh networks", *IEEE ACM Trans. Netw.,* **17**(1), 267-280.

Bahl, P., Adya, A., Padhye, J. and Wolman, A. (2004), "Reconsidering wireless systems with multiple radios", *ACM SIGCOMM Comput. Commun. Rev.*, **34**(5), 39-46.

Campbell, C.E.A., Loo, K.K. and Comley, R. (2010), "A new MAC solution for multi-channel single radio in wireless sensor networks", *ISWCS*, 907-911.

Campbell, C.E.A., Loo, K.K., Gemikonakli, O., Khan, S. and Singh, D. (2011), **"**Multi-channel distributed coordinated function over single radio in wireless sensor networks", *Sensors*, **11**(1), 964-991.

Campbell, C.E.A., Khan, S., Singh, D. and Loo, K.K. (2011), "Multi-Channel Multi-Radio Using 802.11 Based Media Access for Sink Nodes in Wireless Sensor Networks", *Sensors*, **11**(5), 4917-4942.

Cosar, E.I., Bocca, M. and Eriksson, L.M. (2009), "High speed portable wireless data acquisition system for high data rate applications", *Proceedings of the ASME 2009 Int. Design Eng. Tech. Conf. & Comput. and Inf. in Eng. Conf.*, San Diego, California, USA.

Gummeson, J., Ganesan, D., Corner, M.D. and Shenoy, P. (2010), "An Adaptive Link Layer for Heterogeneous Multi-Radio Mobile Sensor Networks", *Proceedings of the IEEE JSAC*, Sept.

Huang, H., Paramo, D. and Dushmukh, S. (2011), "Unpowered wireless transmission of ultrasound signals", *Smart Mater. Struct.*, **20**(1), 015017.

IEEE Std 802.15, (2003), *Standard for part 15.4:wireless medium access control (MAC) and physical layer (PHY) specifications for low rate wireless personal area networks (WPAN).*

Jia, Y., Sun, K., Agosto, F.J. and Quiones, M.T. (2006), "Design and characterization of a passive wireless strain sensor", *Meas. Sci. Technol.*, **17**(11), 2869-2876.

Jurdak, R., Klues, K., Kusy, B., Richter, C., Langendoen, K. and Brunig, M. (2011), "Opal: a multiradio platform for high throughput wireless sensor networks", *IEEE Embedded Syst. Lett.*, **3**(4), 121-124.

Kim, S., Pakzad, S., Culler, D., Demmel, J., Fenves, G., Glaser, S. and Turon, M. (2007), "Health monitoring of civil infrastructures using wireless sensor networks", *Proceedings of the IPSN'07*, Cambridge, Massachusetts, USA.

Kohvakka, M., Arpinen, T., Hannikainen, M. and Hamalainen, T. (2006), "High-performance multi-radio WSN platform", *REALMAN Proceedings of the 2nd ACM Int. Workshop on Multi-hop Ad Hoc Networks: from theory to reality*.

Kuo, V. and Fitch, R. (2011), "A multi-radio architecture for neighbor-to-neighbor communication in modular robots", *Proceedings of the IEEE Int. Conf. on Robot. and Autom.*, Shanghai, China.

Lymberopoulos, D., Priyantha, N.B., Goraczko, M. and Feng, F. (2008), "Towards energy efficient design of multi-radio platforms for wireless sensor networks", *Proceedings of the IPSN: Information Processing in Sensor Networks*.

Lynch, J.P. (2005), "Design of a wireless active sensing unit for localized structural health monitoring", *Struct. Control Health Monit.*, **12**(3-4), 405-423.

Lynch, J.P., Wang, Y., Loh, K., Yi, J.H. and Yun, C.B. (2006), "Wireless Structural Monitoring of the Geumdang Bridge using Resolution Enhancing Signal Conditioning", *Proceedings of the 24th Int. Modal Anal. Conf. (IMAC XXIV).*

Marina, M.K., Das, S.R. and Subramanian, A.P. (2010), "A topology control approach for utilizing multiple channels in multi-radio wireless mesh networks", *Comput. Netw.*, **54**(2), 241-256.
Mascarenas, D.L., Todd, M.D., Park, G. and Farrar, C.R. (2007), "Development of an impedance-based wireless sensor node for structural health monitoring", *Smart Mater. Struct.*, **16**(6), 2137-2145.
Osterlind, F. and Adam, Dunkels. (2008), "Approaching the maximum 802.15.4 multi-hop throughput", *Proceedings of the 5th ACM Workshop on Embed. Networked Sensors*.
Pakzad, S.N., Fenves, G.L., Kim, S. and Culler, D.E. (2008), "Design and implementation of scalable wireless sensor network for structural monitoring", *ASCE J. Infrastruct. Eng.*, **14**, 89-101.
Park, G., Rosing, T., Todd, M.D., Farrar, C.R. and Hodgkiss, W. (2008), "Energy harvesting for structural health monitoring sensor networks", *J. Infrastruct. Syst.*, **14**, 64-79.
Popovici, E., Boyle, D. and O'Connell, S. (2011), "The s-Mote: a versatile heterogeneous multi-radio platform for wireless sensor networks applications", *Proceedings of the 20th Eur. Conf. on Circuit Theory and Des*.
Raman, S., Ganz, A. and Mettu, R.R. (2007), "Fair bandwidth allocation framework for heterogeneous multi-radio wireless mesh networks", *Proceedings of the 4th Int. Conf. on Broadband Commun., Netw. and Syst.*, Raleigh, NC, USA.
SHIMMER Research (2011), "SHIMMER – wireless sensor platform for wearable applications", *available: http://www.shimmerresearch.com*.
So, J. and Vaidya, N.H. (2004), "Multi-channel mac for ad hoc networks: handling multi-channel hidden terminals using a single transceiver" *Proceedings of the 5th ACM MobiHoc*, Tokyo, Japan, May.
Timothy, F., Devinder, M. and Iain, H. (2009), "F-35 joint strike fighter structural prognostics and health management an overview", *Proceedings of the ICAF Conf.*.
Varadan, V.V., Varadan, V.K., Bao, X., Ramanathan, S. and Piscotty, D. (1997), "Wireless passive IDT strain microsensor", *Smart Mater. Struct.*, **6**(6), 745-751.
Wu, J., Yuan, S.F. and Zhao, X. (2007), "A wireless sensor network node designed for exploring a structural health monitoring application", *Smart Mater. Struct.*, **16**(5), 1898-1906.
Wu, J. and Yuan, S.F. (2009), "Design and evaluation of a wireless sensor network based aircraft strength testing system", *Sensors*, **9**(6), 4195-4210.
Zhao, X.L., Qian, T., Mei, G. and Kwan, C. (2007), "Active health monitoring of an aircraft wing with an embedded piezoelectric sensor/actuator network: II wireless approaches", *Smart Mater. Struct.*, **16**(4), 1218-1225.
Zurich, E. (2007), "Btnodes - a distributed environment for prototyping ad hoc networks", *available:http://www.btnode.ethz.ch/*.

JK